# Supporting Information

## Korman et al. 10.1073/pnas.0913531107

### SI Text

**Materials and Methods.** ***Enzyme assays.*** TE/CLC* hydrolytic assays were carried out for the *apo*-mutant and mutants of the catalytic triad residues as previously described and with minor adjustments as noted below (1, 2). Briefly, purified proteins were exchanged into 50 mM potassium phosphate buffer (pH 7.5) on EconoPac 10DG columns (BioRad) according to the manufacturer's instructions. A solution of benzoyl-SNAC (250 mM) in DMSO was prepared for substrate addition. The hydrolysis of a series of concentrations of benzoyl-SNAC was monitored in triplicate after the addition of enzyme (10 μM final), and 100 μl aliquots of the reaction were quenched in 100 μl of 8 M urea at 2, 5, 10, and 15 min followed by incubation on ice. The resulting free thiols were reacted with 5,5′-dithiobis-2-nitrobenzoate (8 mg/ml in ethanol, 8 μl) for 15 min at 20 °C and quantified by UV-visible spectroscopy at 412 nm (1, 2). Reactions were also carried out using a 125 mM benzoyl-SNAC in DMSO solution for substrate addition leading to a 2x higher concentration of DMSO for the enzyme reactions: *apo*-mutant (*apo*-TA1): $k_{cat} = 0.043 \pm 0.0025$ s$^{-1}$, $K_m = 2.61 \pm 0.37$ mM, $k_{cat}/K_m = 0.017 \pm 0.003$ s$^{-1}$/mM$^{-1}$; apo-TA1 (D2070N): $k_{cat} = 0.0345 \pm 0.0017$ s$^{-1}$, $K_m = 2.66 \pm 0.33$ mM, $k_{cat}/K_m = 0.013 \pm 0.002$ s$^{-1}$/mM$^{-1}$; all catalytic triad mutants gave undetectable activity. The added DMSO had little effect on enzyme activity.

***CD analysis.*** Purified proteins from both the *apo*- and *holo*-series were prepared as for the enzyme assays. Concentrations were determined by Bradford assay with bovine albumin as a standard. Proteins were brought to 20 μM final concentration and their CD spectra (JASCO J-710) were collected as the average of three scans.


1. Udwary D, Merski M, Townsend CA (2002) A method for prediction of the locations of linker regions within large multifunctional proteins, and application to a type I polyketide synthase. *J Mol Bio* 323:585–598.
2. Gokhale RS, Hunziker D, Cane DE, Khosla C (1999) Mechanism and specificity of the terminal thioesterase domain from the erythromycin polyketide synthase. *Chem Biol* 6:117–125.


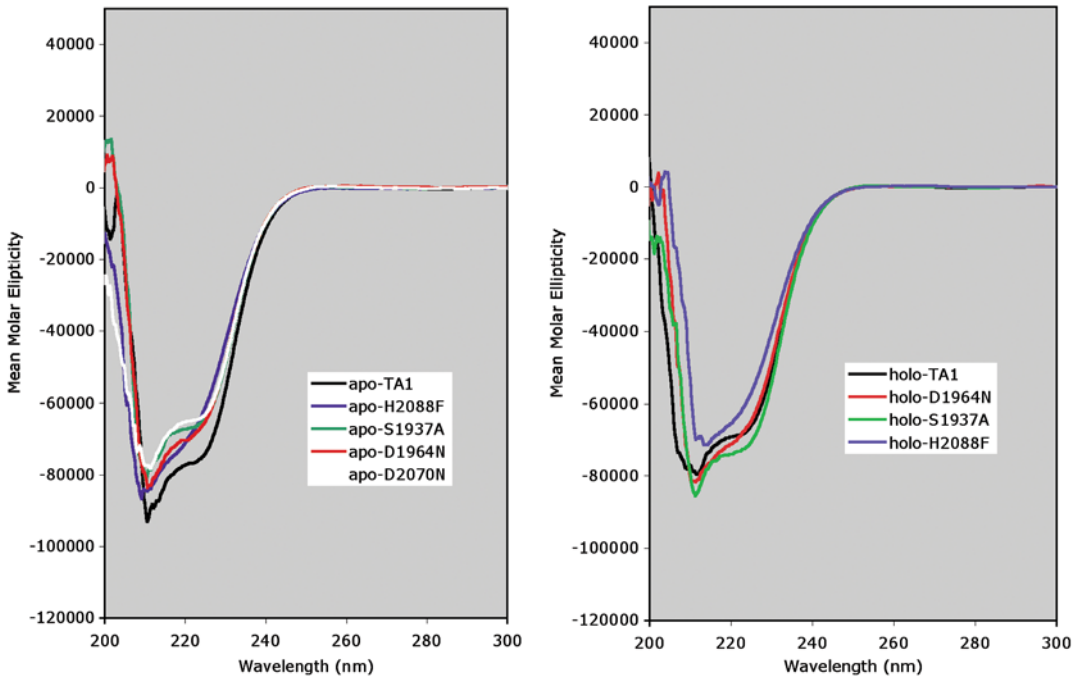


**Fig. S1.** CD spectra for *apo*- (*Left*) and *holo*-ACP-TE (*Right*) didomains and their mutants used in this study.

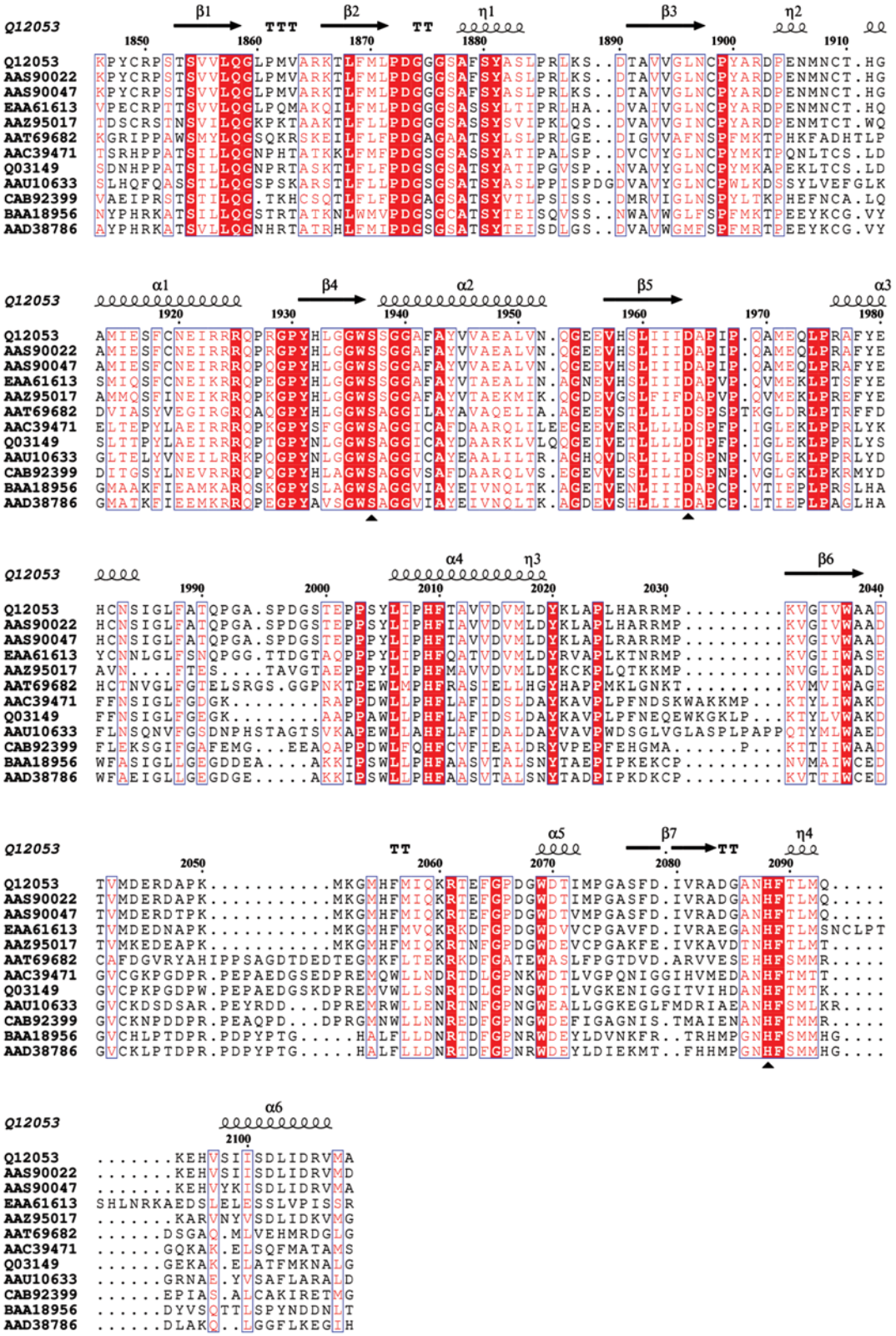


**Fig. S2.** TE/CLC domain alignment. Catalytic triad residues are indicated with a black arrow. See text for critical structural residues involved in binding. Secondary structural elements are shown for PksA TE/CLC from *Aspergillus parasiticus*. TE/CLC sequences consist of *A. parasiticus* PksA (accession number, Q12053; metabolite, aflatoxin), *A. flavus* PksA (AAS90022; aflatoxin), *A. nomius* PksA (AAS90047; aflatoxin), *A. nidulans* STCA (EAA61613; sterigmatocystin), *Mycosphaerella pini* PksA (AAZ95017; dothistromin), *Cercospora nicotianae* CTB1 (AAT69682, cercosporin), *A. fumigatus* Alb1 (AAC39471; naphthopyrone YWA1), *A. nidulans* WA (Q03149; naphthopyrone YWA1), *Gibberella zeae* PKS12 (AAU10633; aurofusarin), *Gibberella fujikuroi* PKS4 [CAB92399 updated sequence (1); bikaverin], *Colletotrichum lagenarium* PKS1 (BAA18956; melanin), and *Nodulisporium sp.* ATCC74245 PKS1 (AAD38786; melanin).

1. Crawford JM, Vagstad AL, Whitworth KP, Ehrlich KC, Townsend CA (2008) Synthetic strategy of nonreducing iterative polyketide synthases and the origin of the classical "starter-unit effect." *ChemBioChem* 9:1019-1023.

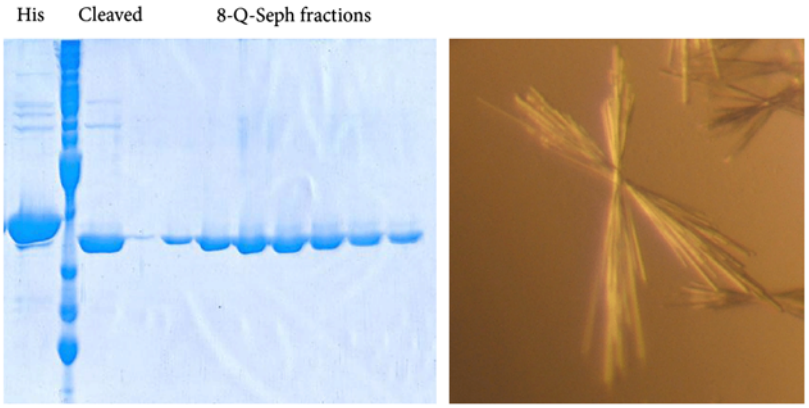


**Fig. S3.** SDS-PAGE image for the TE/CLC monodomain purification (His, $His_6$-tagged construct; Cleaved, protein after thrombin treatment; and Q-Seph, 8-fractions enriched after anion exchange chromatography). Image of TE/CLC mondodomain crystal.

**Table S1. Data collection, MAD, and refinement statistics**

| | | SeMet TE | | |
|---|---|---|---|---|
| | Native PksA TE | Peak | Inflection | Remote |
| *Data Collection* | | | | |
| Wavelength (Å) | 1.0 | 0.98 | 0.98 | 1.2 |
| Space Group | $P2_12_12_1$ | | $P2_12_12_1$ | |
| Cell Dimensions | | | | |
| *a* (Å) | 66.93 | | 66.91 | |
| *b* (Å) | 66.94 | | 67.13 | |
| *c* (Å) | 67.92 | | 67.80 | |
| Resolution Range (Å) | 50-1.7 | 50-3.0 | 50-3.1 | 50-3.0 |
| No. of Observations | 402056 | 269924 | 269977 | 274209 |
| No. of Unique Reflections | 34357 | 6539 | 5937 | 6510 |
| Redundancy | 6.6 | 11.2 | 11.2 | 12.2 |
| Completeness (%) (last shell) | 99.9 (99.2) | 98.7 (90) | 98.7 (90.8) | 99.8 (99) |
| Mean $I/\sigma(I)$ (last shell) | 40.7 (5.7) | 13 (4.5) | 13.2 (4.1) | 16.5 (6.7) |
| $R_{merge}$ (last shell) | 5.7 (29.5) | 19.1 (28.1) | 18.9 (32.1) | 18.5 (29.6) |
| MAD phasing | | | | |
| Resolution Range (Å) | | | 50-3.5 | |
| Number of Derivative Sites | | | 13 | |
| FOM | | | 0.5 | |
| *Refinement* | | | | |
| Resolution Range (Å) | 50-1.7 | | | |
| No. of Reflections | 33560 | | | |
| No. of Protein Atoms | 2042 | | | |
| No. of Waters | 170 | | | |
| $R_{crys}$ (%) | 18 | | | |
| $R_{free}$ (%) | 20 | | | |
| *Geometry* | | | | |
| RMSD for Bonds (Å) | 0.0058 | | | |
| RMSD for Angles (deg) | 1.31 | | | |
| RMSD for *B* Main Chain | 1.005 | | | |
| RMSD for *B* Side Chain | 1.55 | | | |
| Ramachandran Plot (%) | | | | |
| most favored | 90.5 | | | |
| favored | 8.5 | | | |
| generously allowed | 1.0 | | | |
| disallowed | 0 | | | |